Dynamic Analysis and Damage of Composite Layered Plates Reinforced by Unidirectional Fibers Subjected Low Velocity Impact

Josef Soukup, Milan Zmindak, Pavol Novak, Frantisek Klimenda, Michal Kaco, and Lenka Rychlikova

Abstract Currently, for dynamic modeling in composite structures at low and high speeds are used mainly Finite Element Method (FEM). For these analyzes commercial FEM software ABAQUS/explicit, LS-DYNA, AUTODYN and PAM CRASH, etc., are used in practice. In the present study, low-velocity impact response of composite laminates was studied using ABAQUS/Explicit code (FEM) to investigate damage by employing various damage criteria. The basic material properties in and transverse to the fiber directions, such as the elastic moduli, strains at failure, and plastic moduli among others are determined by simple tests in tension, compression, and shear. The material properties AS4/PEEK was used in numerical simulations and have been taken from the literature. Layer is considered as homogeneous transversely isotropic and layer stacking sequence is symmetrical or unsymmetrical. The solution in the form of time integration can be, depending on the problem, accomplished via implicit or explicit methods. For many of dynamic problems explicit methods have shown more suitable, cause they do not require stiffness, mass and damping matrix decomposition. In the plates examined, von Mises's stress and damage caused shear stress in the matrix and fiber were evaluated. From the results obtained, it was found that the von Mises stress was approximately the same for all types layer stacking sequence.

Keywords FEM · ABAQUS · Composite material

J. Soukup (✉) · F. Klimenda · L. Rychlikova
Faculty of Mechanical Engineering, University of J. E. Purkyne in Usti nad Labem, Usti nad Labem, Czech Republic
e-mail: josef.soukup@ujep.cz

M. Zmindak · P. Novak · M. Kaco
Faculty of Mechanical Engineering, University of Zilina, Zilina, Slovak Republic

J. Awrejcewicz (ed.), *Perspectives in Dynamical Systems II: Mathematical and Numerical Approaches*, Springer Proceedings in Mathematics & Statistics 363,
https://doi.org/10.1007/978-3-030-77310-6_15

1 Introduction

Fiber reinforced polymers (FRP) are most commonly used materials in various fields of industry. In the recent years quickly developing industries such as aerospace, ship and car industry almost completely rely on composite materials, especially on layered polymers reinforced with glass, aramid or carbon fibers and sandwich constructions consisting of FRP coatings with a foam core. Such constructions offer high strength at low weight, which considerably improve their performance (higher loading capacity, lower fuel consumption, etc.) especially in ship and aerospace industry [1, 2]. These materials also have good antiballistic properties, for example modern bulletproof vests are made from aramid fibers.

The most important characteristic of the composite materials is that they can be layered, with the fibers in each layer running in a different direction. This allows an engineer to design structures with unique properties, furthermore a structure can be designed so that it will bend in one direction, but not another. Impact damage is one of the main problems that composite structures face, there needs to be a way of reducing that damage when it occurs, reducing it enough so that the integrity of the structure is not comprised.

Today, typically, numerical models based on lamina-level failure criteria are used to simulate the damage of the fiber-reinforced composite material, although with well-accepted limitations. In this constitutive models, composite, are modelled as orthotropic linear elastic materials within the failure surface. The failure surface is defined by the failure criterion as maximum stress/strain criterion, Hashin's criterion, Christensen's criterion, Chang-Chang's criterion, Puck's criterion, LARC, etc. [3, 4].

They are many definition of low velocity or low energy impact due of the great number of parameters that should be study such as the velocity, the shape and the mass of the impactor [5]. The dynamical response of the structure depends therefore on the duration of the contact between the structure and the impactor. Cantwell and Morton [6] have proposed that every dynamic solicitation corresponding to an impact speed below 10–20 m/s can be considered as a low velocity impact. On other hand, Abrate [7] considers that the impact speed limit defining a low velocity impact is five to ten time greater than the one proposed by Cantwell and Morton (100 m/s). Liu et al. [8] uses a different approach based on the internal damage of the impacted structure. They postulate that a high velocity impact leads to fibres rupture where as low velocity impact leads to internal delamination and matrix cracking.

2 Theory Background and Solution Method

The contact between two components or bodies is a static phenomenon if the two bodies are static equilibrium. Otherwise the contact is a dynamic phenomenon. A dynamic contact is often much complicated than static one. The term 'contact-

impact' is often used to stress the dynamic effects in contact phenomena [9, 10]. By nature, contact phenomena always involve friction phenomena. However, friction effects may be neglected in situations where frictional forces are sufficiently small. Therefore, we may have a frictionless contact, which is a special case of general contact. Mechanical problems involving contact are inherently non-linear and contact problems involve unknown boundary conditions.

2.1 Transient Stress Analysis

Figure 1 shows the transient analysis model of laminate and punch. At the t moment, the equilibrium equation can be deduced as:

$$\sigma_{ij,j}^{t} = \rho^{t}\ddot{u}_i + \mu^{t}\dot{u}_i \tag{1}$$

where ρ^t and μ^t are the density and dynamic friction coefficient of laminate at t moment, respectively.

$$\sigma_{ij}^{t} n_j - \overline{T}_i^{t} = 0 \ \ (\text{on } S_\sigma) \tag{2}$$

where, S_σ represents the stress boundary.

The equivalent integration of the equilibrium equation and the load boundary condition can be expressed, as follows:

$$\int_V \delta u_i \left(\sigma_{ij,j}^{t} - \rho^{t}\ddot{u}_i - \mu^{t}\dot{u}_i\right) dV - \int_{S_\sigma} \delta u_i \left(\sigma_{ij}^{t}\, n_j - \overline{T}_i^{t}\right) dS = 0 \tag{3}$$

As there will be geometric nonlinearity during the deformation of composite under the low-velocity impact load, strain tensor at the t moment can be expressed, as follows [11, 12]:

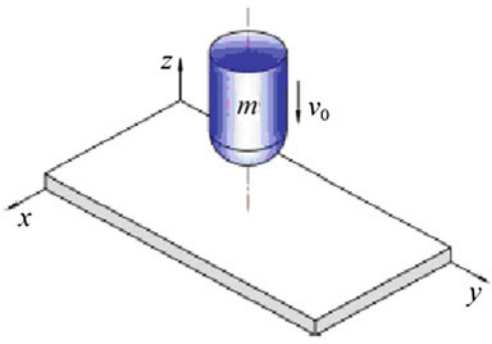

Fig. 1 Transient analysis model of laminate and punch

$$\varepsilon_{ij}^{t} = \frac{1}{2}\left(u_{i,j}^{t} + u_{j,i}^{t} + u_{k,i}^{t}\, u_{k,j}^{t}\right), (i, j, k = x, y, z) \tag{4}$$

Decompose the above equation in to linear and nonlinear terms

$$\varepsilon = \varepsilon_L + \varepsilon_{NL} \tag{5}$$

There is the following relationship of σ_{ij}^{t} and ε_{kl}^{t} at t moment

$$\sigma_{ij}^{t} = \overline{Q}_{ijkl}^{\,t-\Delta t} + \varepsilon_{kl}^{t} \tag{6}$$

where $\overline{Q}_{ijkl}^{\,t-\Delta t}$ represents material elasticity matrix at $t - \Delta t$ moment, and it can be obtained by coordinate transformation [13]

$$\overline{Q}_{ijkl}^{\,t-\Delta t} = [T]\ Q^{\,t-\Delta t}[T]^{T} \tag{7}$$

Using Eqs. (3) and (6), the stress equilibrium equation at each moment can finally be deduced as

$$\int \left(\delta\varepsilon_{ij}\ \overline{Q}_{ijkl}^{\,t-\Delta t}\varepsilon_{kl} + \delta u_i\ \rho^{t}\ddot{u}_i + \delta u_i\ \mu^{t}\dot{u}_i\right) dV + \int_{V_{n-1}} \sigma_{ij}^{n-1}\delta\left(\Delta\eta_{ij}\right) dV = \int_{S_\sigma} \overline{T}_i^{n}\ \delta u_i\ dS \tag{8}$$

where $\overline{T}_i^{t}$ and $\overline{T}_i^{n}$ are the surface force at t moment and nth step in numerical analysis respectively; $\delta\varepsilon_{ij}$ represents the strain at t moment; and, $\Delta\eta_{ij}$ is the nonlinear term of strain increment.

2.2 Solution Methods

Recently the most successful method for modeling the dynamic response of a structure is FEM [14]. The solution in the form of time integration can be, depending on the problem, accomplished via implicit or explicit methods. Although implicit methods are unconditionally stable (they are not dependent on the time step size), for wave propagation problems explicit methods have shown more suitable, cause they do not require stiffness, mass and damping matrix decomposition. The system of equations has the form

$$\mathbf{M}\ddot{\mathbf{u}}_{(t)} + \mathbf{C}\dot{\mathbf{u}}_{(t)} + \mathbf{K}\mathbf{u}_{(t)} = \mathbf{F}_{(t)}^{\text{ext}} \tag{9}$$

The solution of this system is carried out for each time step via the explicit central difference method. Here, the acceleration in time t has the form

$$\ddot{\mathbf{u}}_{(t)} = \mathbf{M}^{-1}\left[\mathbf{F}_{(t)}^{ext} - \left(\mathbf{C}\dot{\mathbf{u}}_{(t)} + \mathbf{K}\mathbf{u}_{(t)}\right)\right] = \mathbf{M}^{-1}\left[\mathbf{F}_{(t)}^{ext} - \mathbf{F}_{(t)}^{\text{int}}\right] \tag{10}$$

where $\boldsymbol{F}_{\boldsymbol{t}}^{\boldsymbol{ext}}$ is the vector of external forces and $\boldsymbol{F}_{\boldsymbol{t}}^{\boldsymbol{int}}$ is the vector of internal forces gives as

$$\mathbf{F}_{t}^{\text{int}} = \sum\left(\int_{\Omega}\left(\mathbf{B}^{T}\sigma_{n}d\Omega + F^{hg}\right)\right) + F^{cont} \tag{11}$$

Velocities and accelerations have the form

$$\Delta t^{2}\ddot{\mathbf{u}}_{(\mathrm{t})} = \mathbf{u}_{(\mathrm{t}-\Delta\mathrm{t})} - 2\mathbf{u}_{(\mathrm{t})} + \mathbf{u}_{(\mathrm{t}+\Delta\mathrm{t})} \tag{12}$$

$$2\Delta t\ \dot{\mathbf{u}}_{(\mathrm{t})} = \mathbf{u}_{(\mathrm{t}+\Delta\mathrm{t})} - \mathbf{u}_{(\mathrm{t}-\Delta\mathrm{t})} \tag{13}$$

The starting procedure has the form

$$\mathbf{u}_{(\mathrm{t}-\Delta\mathrm{t})} = \mathbf{u}_{(0)} - \Delta t\dot{\mathbf{u}}_{(0)} + \frac{\Delta t^{2}}{2}\ddot{\mathbf{u}}_{(0)} \tag{14}$$

By applying zero initial conditions to the displacements and velocities, the starting procedure has the form

$$\ddot{\mathbf{u}}_{(t-\Delta t)} = \mathbf{M}^{-1}\mathbf{F}_{(\mathbf{0})}^{\mathbf{ext}} \tag{15}$$

The stability of the central difference method depends on the length of the time step, which has to be divided into the shortest natural domains in the finite element mesh. The critical time step is computed by following relation

$$\Delta t^{crit} = \frac{2}{\omega_{\max}} \tag{16}$$

where ω_{max} is the maximum natural circular frequency. The calculation is based on Courant-Friedrichs-Lewy condition (CFL condition) for solving partial differential equations numerically by the method of finite differences

$$\omega_{\max} = 2\frac{\mathrm{c}}{1} \tag{17}$$

where c is the wave speed in the material and l is the characteristic length. By substitution (Eq. 9) into (Eq. 7) we obtain relation for critical time step

$$\Delta t = \frac{l}{c} \tag{18}$$

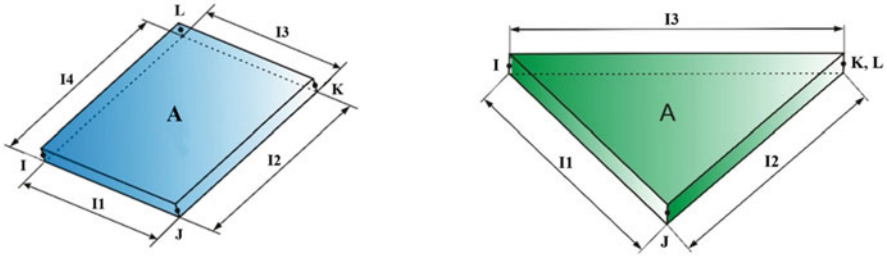

Fig. 2 Quadrilateral and triangular shell element

where Δt is time required for wave propagation in rod with length l. During time step calculation, ABAQUS/explicit program check size of all finite elements. For the numerical stability of calculation was used coefficient 0.9 for time step reduction

$$\Delta t = 0.9\frac{l}{c}x \tag{19}$$

Characteristic length of a shell element is given as

$$l = \frac{A}{\max\left(l_1, l_2, l_3, l_4\right)} \tag{20}$$

where A is the element area, l_i are lengths sides of Fig. 2. For triangular shell element the relation has the form

$$l = \frac{2A}{\max\left(l_1, l_2, l_3\right)} \tag{21}$$

Wave propagation velocity in a shell element is given by relation

$$c = \sqrt{\frac{E}{\rho\left(1-\mu^2\right)}}x \tag{22}$$

where E is the Young modulus, ρ is mass density and μ is the Poisson number.

3 Description of Problem and Modelling Approach

Today, typically, finite element numerical models based on lamina-level failure criteria are used to simulate the damage of the fiber-reinforced composite material. Damage modeling usually encompasses two phases: damage initiation and damage evolution.

3.1 Materials

In the present paper, Hashin's criterion is implemented to identify fiber and matrix failure initiation. This criterion involves four damage modes, namely, fiber tension, fiber compression, matrix tension and matrix compression modes according to the following equations:

1. Fiber tensile failure: $\left(\hat{\sigma}_{11} \geq 0\right)$:

$$\left(\frac{\hat{\sigma}_{11}}{X_T}\right)^2 + \frac{\hat{\sigma}_{12}^2 + \hat{\sigma}_{13}^2}{S_{12}^2} = \begin{cases} \geq 1 & \text{failure} \\ < 1 & \text{no failure} \end{cases} \tag{23}$$

2. Fiber compressive failure $\left(\hat{\sigma}_{11} < 0\right)$:

$$\left(\frac{\sigma_{11}}{X_C}\right)^2 = \begin{cases} \geq 1 & \text{failure} \\ < 1 & \text{no failure} \end{cases} \tag{24}$$

3. Matrix tensile failure $\left(\hat{\sigma}_{22} \geq 0\right)$:

$$F_{mt} = \left(\frac{\hat{\sigma}_{22}}{Y^T}\right)^2 + \left(\frac{\hat{\sigma}_{12}}{S_{12}}\right)^2 = 1 \tag{25}$$

4. Matrix compressive failure $\left(\hat{\sigma}_{22} < 0\right)$:

$$F_{mc} = \left(\frac{\hat{\sigma}_{22}}{2S_{23}}\right)^2 + \left[\left(\frac{Y^C}{2S_{23}}\right)^2 - 1\right]\frac{\hat{\sigma}_{22}}{Y^C} + \left(\frac{\hat{\sigma}_{12}}{S_{12}}\right)^2 = 1 \tag{26}$$

where, σ_{ij} $\widehat{\sigma}_{ij}$ are effective stress, X^T and X^C are tensile and compressive strength of composite laminate in fiber direction, Y^T and X^C are tensile and compressive strength in transverse direction, S_{12} and S_{23} are longitudinal and transverse shear strength of the composite, respectively. The coefficient α is for shear stress contribution on the fiber tensile failure.

The material of present composite is an AS4/PEEK quasi-isotropic laminate. For the simulation of impact damage has been used four types of orientation layers (layup):

$$\left[\begin{matrix}0\\0\\0\\0\end{matrix}\right]_S, \left[\begin{matrix}0\\0\\90\\90\end{matrix}\right]_S, \left[\begin{matrix}45\\45\\45\\45\end{matrix}\right]_S \tag{27}$$

Material parameters of the laminate plate are listed in Tables 1 and 2.

Table 1 Material properties of AS4/PEEK

E_{11} (GPa)	E_{22} (GPa)	ν_{12} (–)	G_{12} (GPa)	G_{13} (GPa)	G_{23} (GPa)	ρ (kg/m^3)	X_T (MPa)	X_C (MPa)
138	10.2	0.3	5.7	5.7	3.7	1570	2070	1360
Y_T (MPa)	Y_C (MPa)	S_L (MPa)	S_T (MPa)					
86	230	186	86					

Table 2 Fracture energy of laminate (course of damage) [15]

	F_f^t	F_f^c	F_m^t	F_m^{tc}
Fracture energy (N/mm)	12.5	12.5	1.0	1.0

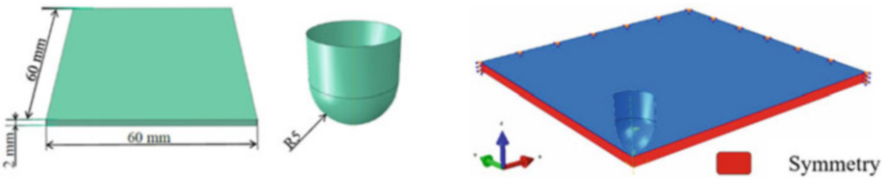

Fig. 3 Geometry of composite plate and impactor (to the left), boundary conditions (to the right)

Fig. 4 Finite element mesh of conventional shells

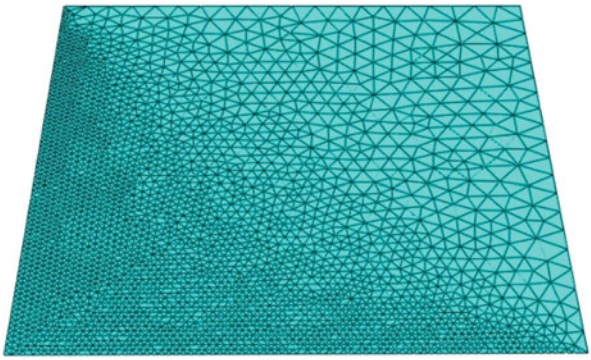

3.2 Finite Element Modeling

In the next simulations were considered composite plate with dimensions 120 × 120 × 2 mm composed from eight layers. Due to the symmetry, only quarter of the geometry was modelled to save the computational cost (Fig. 3). The composite plate structure was created in ABAQUS/explicit using the composite module [16]. This module involves the formation of conventional and volumetric shells (Figs. 4 and 5). This module defines the individual layers of the composite structure, the type of integration rule, symmetry, material properties, thickness, orientation and the number of integration points of the layer.

The composite plate is composed from the eight-node brick hexahedral elements with one integration point (C3D8R) and 50,000 elements were used in the simula-

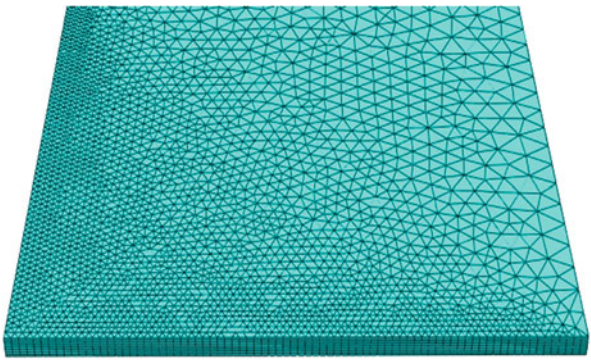

Fig. 5 Finite element mesh of volumetric shells

tion. A refined, uniform mesh was used in the impact region. The ABAQUS/Explicit simulations presented here examined the penetration of plate specimens.

The projectile has cylindrical shape with semi-spherical fillet with a radius $R = 5$ mm. Since results from ballistic experiments showed negligible deformation, plastic deformation of the projectile is not considered. The projectile impacts the plate perpendicularly, right is center of the plate with a defined initial speed $v_i =$ 100 m/s and the plate was supported on all edges. FE mesh for the shell geometry was created using 5450 linear triangular elements S3R and for solid geometry has been used 39.520 linear SC6R brick elements (Fig. 5).

The composite structure consists of 8 layers, one layer having a thickness of 0.25 mm. The number of integration points has been set by default. The following four types of layer orientation were used to simulate the impact damage (27).

4 Result

The ABAQUS/Explicit simulations presented here examined the penetration of composite plate samples impacted with steel rod with a hemispherical. Figures 6 and 7 show the dependence of acceleration and velocity on time at the node where is maximum displacement. The maximum value of acceleration is $5.2e^{+08}$ m/s^2 and maximum value of velocity is 139 m/s.

In the volumetric shell geometry, the maximum stress was von Mises 2090 MPa and the shear damage occurred only in the area close to the impactor impact (Fig. 8). In conventional shell geometry, damage propagate from the impact point to the edge of tested plate, and shear damage also occurred at the edges of the plate. The maximum von Mises stress reached 2100 (Fig. 9).

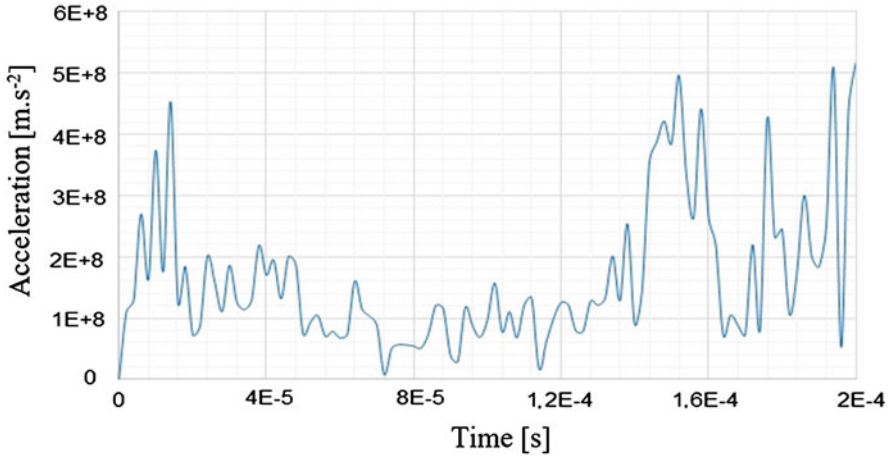

Fig. 6 Time history of acceleration at node with maximum displacement

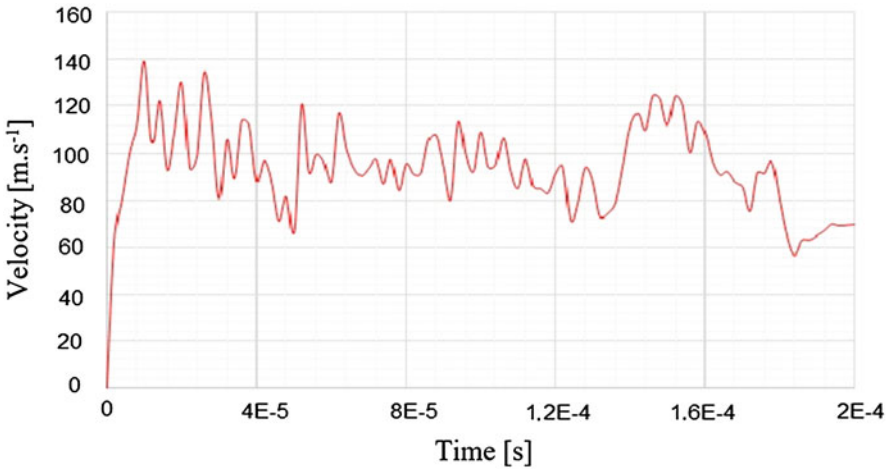

Fig. 7 Time history of velocity at maximum displacement

5 Conclusion

In this paper for the analysis of laminate composite plates two models are used. The first is the solid based model and other is shell based model. There were also compared four different arrangement of the layers of the composite. As a criterion damage the composite plate was used Hashin damage model. The results obtained show that the von Mises stress have approximately the same value for all types of arrangements of the layers. For solid model, and also for the shell model was the largest von Mises stress in the arrangement of layers $[0/0/90/90]_s$

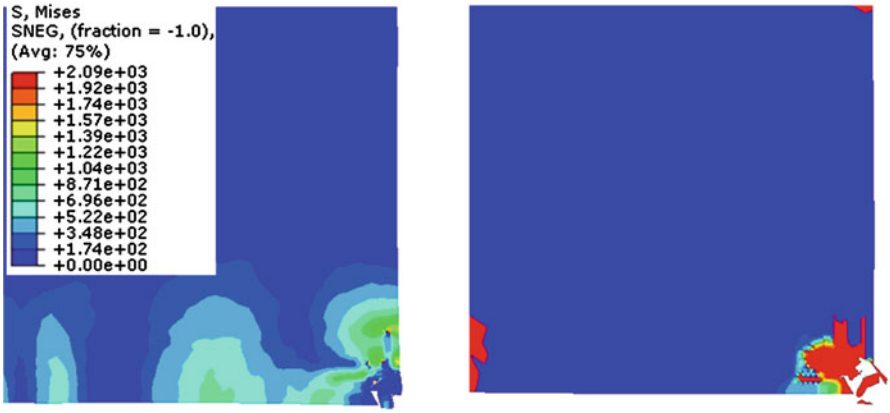

Fig. 8 Course of von Mises stress (to the left) and shear stress (to the right) for volumetric shell geometry—$[0/0/90/90]_s$

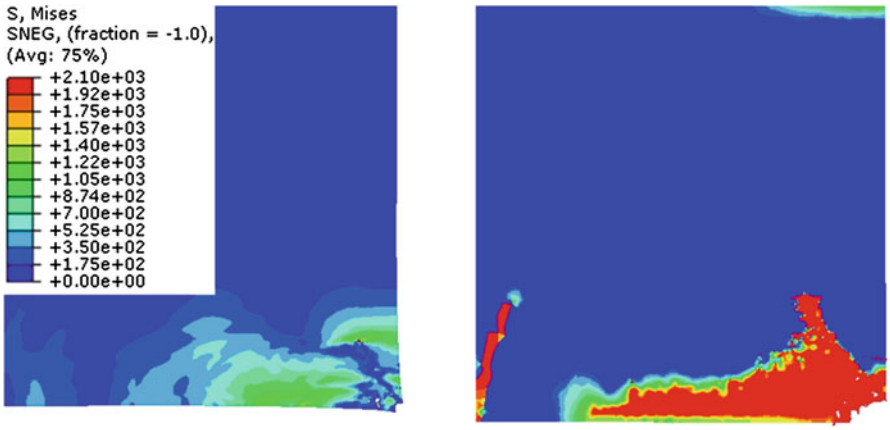

Fig. 9 Course of von Mises stress (to the left) and shear stress (to the right) for conventional shell geometry—$[0/0/90/90]_s$

the lowest von Mises stress was in the arrangement of the layers $[90/0/0/0]_s$. For the arrangement of layers $[90/0/0/0]_s$, $[45/45/45/45]_s$ is the lowest von Mises stress for shell based model. The largest shear stresses were in the arrangement of the layers $[45/45/45/45]_s$ for solid as well as shell based model. The largest deformation was at the area of impact, which gradually propagate to the depth of the material. From the results we can see that the orientation of the layers in the composite structures can have a significant effect on the behavior of the structure.

Acknowledgments This work was supported by internal grant of Jan Evangelista Purkyně, Faculty of Mechanical Engineering (UJEP-IGS-2018-48-002-1 and UJEP-SGS-2018-48-002-2).

References

1. Barbero, E.J.: Introduction to Composite Materials Design. CRC Press, Boca Raton (2011)
2. Marulo, F., Guida, M., Maio, L., Ricci, F.: Numerical simulation and experimental experiences of impact on composite structures. In: Dynamic Response and Failure of Composite Materials and Structures. Woodhead Publishing, Duxford (2017)
3. Barbero, E.J.: Finite Element Analysis of Composite Materials Using ABAQUS. CRC Press, Boca Raton (2013)
4. Zhang, H., Wang, M., Wen, W., Xu, Y., Cuiu, H., Chen, J.: A full-process numerical analyzing method of low velocity impact damage and residual strength for stitched composites. Appl. Sci. **8**, 2698 (2018). https://doi.org/10.3390/app8122698
5. Dong, S., Sheldon, A., Carney, K.: Modeling of carbon-fiber-reinforced polymer (CFRP) composites in LS-dyna with optimization of material and failure parameters in LS-OPT. In: 15th International LS-DYNA Users Conference, 10–12 June 2018, Detroit, MI, USA
6. Cantwell, W.J., Morton, J.: The impact resistance of composite materials—a review. Composites. **22**, 347–362 (1991)
7. Abrate, S.: Impact Engineering of Composite Structures. Springer, Udine (2011)
8. Liu, D., Malvern, L.E.: Matrix cracking in impacted glass/epoxy plates. J. Compos. Mater. **21**, 594–609 (1987)
9. Zhong, Z.-H.: Finite Element Procedures for Contact-Impact Problems. Oxford University Press, Oxford (1993)
10. Wriggers, P.: Computational Contact Mechanics. Antony Rowe Ltd., Chippenham (2002)
11. Bathe, K.J.: Finite Element Procedures. Prentice-Hall Inc., Englewood Cliffs, NJ (1995)
12. Crisfield, M.A.: Non-linear Finite Element Analysis of Solids and Structures. Essentials, vol. 1. John Wiley & Sons Ltd., Chichester (2000)
13. Belytschko, T., Liu, W.K., Moran, B.: Nonlinear Finite Elements for Continua and Structures. John Wiley & Sons Ltd., Chichester (2000)
14. Ibrahimbegovic, A.: Nonlinear Solid Mechanics, Theoretical Formulations and Finite Element Solution Methods. Springer, New York (2009)
15. Nanderi, M., Khonsari, M.M.: Ch. 4: Stochastic analysis of inter- and intra-laminar damage in notched PEEK laminates. In: EBSCO HOST Connection. Online version, vol. 7, p. 383. Louisiana State University (2013)
16. ABAQUS. Theory manual version 6.10. Documentation [online]. 2015. [cit. 10.03.2015]. Available from: <http://abaqusdoc.ucalgary.ca/books/stm/default.htm> (2010)